River network-scale drying impacts the spatiotemporal dynamics of greenhouse gas fluxes

Teresa Silverthorn, Naiara López-rojo, Romain Sarremejane, Arnaud Foulquier, Vincent Chanudet, Abdelkader Azougui, Rubén del Campo, Gabriel Singer, Thibault Datry

River network-scale drying impacts the spatiotemporal dynamics of greenhouse gas fluxes

Teresa Silverthorn [1]*, Naiara López-Rojo [1,2] Romain Sarremejane, [1,a] Arnaud Foulquier, [2] Vincent Chanudet, [3] Abdelkader Azougui, [1] Rubén del Campo [4] Gabriel Singer, [4] Thibault Datry [1]

[1]National Institute for Agriculture, Food, and Environment (INRAE), RiverLy Research Unit, Centre de Lyon-Grenoble Auvergne-Rhône-Alpes, Villeurbanne, France
[2]Univ. Grenoble-Alpes, Univ. Savoie Mont Blanc, CNRS, LECA, Grenoble, France
[3]HYNES (Irstea—EDF R&D), Savoie Technolac, Électricité de France (EDF), Hydro Engineering Centre, Department ES, France
[4]Department of Ecology, University of Innsbruck, Innsbruck, Austria

Abstract

Rivers significantly contribute to global biogeochemical cycles; however, we have a limited understanding of how drying may influence these cycles. Drying fragments river networks, thereby influencing important ecosystem functions such as the processing of carbon and nitrogen, and associated fluxes of greenhouse gases (GHGs) both locally, and at the river network scale. Our objective was to assess, using a network-scale approach, the lateral, longitudinal, and temporal dynamics of GHG fluxes in a river network naturally fragmented by drying. We used a closed-loop chamber with automated analyzers to measure carbon dioxide (CO_2), methane (CH_4), and nitrous oxide (N_2O) fluxes from dry sediments, flowing waters, isolated pools, and riparian soils, along with a suite of environmental variables, over 9 months at 20 sites across a non-perennial river network in France. Network-scale drying had a spatial and temporal legacy effect on GHG fluxes. On average, CO_2 fluxes were up to 29 times higher from perennial than non-perennial sites under flowing conditions. At non-perennial sites, CO_2 and N_2O fluxes positively covaried with time since rewetting. In addition, CO_2 and N_2O fluxes at perennial sites positively covaried with the percent of non-perennial reaches upstream, indicating a spatial effect of drying. GHG fluxes from riparian soil and dry riverbed sediments had markedly different magnitudes and covariates. This research demonstrates that drying not only has a local-scale impact but also influences GHG fluxes at the network scale, contributing valuable insights for upscaling global riverine GHG estimates.

Relative to their spatial extent in the landscape, river networks contribute disproportionately to global biogeochemical cycles (Cole et al. 2007; Battin et al. 2009; Raymond et al. 2013; Allen and Pavelsky 2018). Rivers receive large amounts of terrestrially derived carbon (C) that are subsequently stored,

transformed, or ultimately transported to the ocean (Cole et al. 2007; Battin et al. 2008). Globally, carbon dioxide (CO_2) evasion from streams and rivers, driven by mineralization of terrestrial organic C inputs, in-stream primary production, as well as groundwater inputs of inorganic C (Hotchkiss et al. 2015), were estimated to be five times higher than those from lakes and reservoirs (Raymond et al. 2013). The magnitudes and drivers of greenhouse gas (GHG) fluxes in rivers are altered in the face of global change. For example, augmented terrestrial subsidies enhance C outgassing from inland waters (Regnier et al. 2022), and an increased occurrence of droughts can increase water residence times, promoting anaerobic conditions associated with methane (CH_4) production (Gómez-Gener et al. 2020). In addition, anthropogenic nitrogen (N) inputs to fluvial systems may result in outgassing the equivalent of 10% of global anthropogenic nitrous oxide (N_2O) emissions (Beaulieu et al. 2010). The effects of anthropogenic influences on biogeochemical cycling in rivers are complex due to the manifold and interacting controls on GHG fluxes at different spatial and temporal scales. Yet, it is critical to improve our understanding of the drivers of these

Additional Supporting Information may be found in the online version of this article.

fluxes across scales to better predict riverine C sequestration and GHG fluxes (Battin et al. 2023).

The vast majority of river networks on Earth dry naturally (Messager et al. 2021) and due to global change (Datry et al. 2023), but it remains largely unknown how drying events influence the dynamics of GHG fluxes across river networks (Battin et al. 2023). The proportion of drying river networks, wherein surface water ceases to flow for some period of time, is likely to increase with climate change, damming, and water abstraction (Zipper et al. 2021; Datry et al. 2023). Drying has local effects on biodiversity (Leigh and Datry 2017), nutrient cycling (Shumilova et al. 2019), and GHG fluxes (Gómez-Gener et al. 2016). Drying may also act as a fragmentation agent with regional effects at the river network scale. For example, the fragmentation of river networks by drying alters connectivity and, hence, the space–time organization of regional biodiversity (Gauthier et al. 2020; Jacquet et al. 2022). Similarly, drying can alter C fluxes at the river network scale by facilitating large downstream pulses of poorly decomposed accumulated organic matter (OM) associated with hot moments of CO_2 emission upon rewetting (Datry et al. 2018). While there has been progress in understanding the local effects of drying on GHG fluxes (e.g., Gómez-Gener et al. 2016), the regional effect of the fragmentation of river networks by drying is still overlooked.

Our knowledge of the local-scale drivers of GHG fluxes from dry riverbeds has expanded in recent years. CO_2 efflux is higher on average from dry riverbed sediments than from flowing waters in arid climates (von Schiller et al. 2014; Gómez-Gener et al. 2015, 2016; Looman et al. 2017). This difference in CO_2 efflux may be attributed to the oxygenation of sediments promoting OM degradation while water is no longer limiting gas diffusion (Kosten et al. 2018). The underlying local-scale drivers of dry sediment GHG fluxes include sediment moisture, sediment temperature, and sediment OM content for CO_2 (Gómez-Gener et al. 2016; Bolpagni et al. 2017; Keller et al. 2020), with limited data available for CH_4 (but *see* Paranaíba et al. 2021) and N_2O (but *see* Gallo et al. 2014), two gases with high global warming potentials (Myhre et al. 2013). Recent global scale studies have demonstrated the importance of CO_2 (Keller et al. 2020) and CH_4 (Paranaíba et al. 2021) fluxes from dry inland waters. However, these estimates were generally derived from snapshots in time and do not account for the dynamic and complex nature of dendritic river networks. Moreover, only a few studies include measures of GHG fluxes from isolated pools in dry rivers (von Schiller et al. 2014; Gómez-Gener et al. 2015), despite their high potential for methanogenesis and denitrification due to an accumulation of OM and sediments paired with high water residence time (Wang et al. 2018).

In addition to considering local drivers of GHG fluxes, a river network-scale approach is needed to better understand how drying alters biogeochemical cycling in rivers. Through fragmentation by drying, the interruption of surface flow disrupts hydrological connectivity in one or more of the vertical (from the surface to the subsurface), lateral (from the riparian zone to the in-stream habitat), and longitudinal (from upstream to downstream) dimensions, creating heterogeneous mosaics of habitat patches with varying conditions over space and time (Datry et al. 2016; Cid et al. 2021). The spatial distribution of drying was shown to affect metabolic activities and associated dissolved oxygen concentration patterns (Diamond et al. 2023), however less is known about its effect on other biogeochemical processes and particularly GHG fluxes. In the temporal dimension, drying may leave a legacy effect on flowing-condition GHG fluxes through its effects on particulate OM accumulation and decomposer communities. OM may accumulate in dry reaches, providing plentiful substrate for metabolism upon rewetting, locally and for downstream reaches (Datry et al. 2018; Catalàn et al. 2023). In parallel, drying may impair the structure and functioning of microbial and invertebrate decomposer communities (Foulquier et al. 2015; Truchy et al. 2020; Schreckinger et al. 2021, 2022), even long after flow resumption (Datry et al. 2011; Gauthier et al. 2020; Di Sabatino et al. 2022). The lateral connection between the stream and the riparian zone is also fundamental for riverine biogeochemical cycling (Covino 2017). For example, lateral groundwater inputs enriched in dissolved OM enhance heterotrophic activity in streams (Lupon et al. 2023). The strength of this connection varies with network position as headwater streams have proportionally greater importance of terrestrially derived CO_2 than in-stream production when compared to downstream reaches (Hotchkiss et al. 2015). Understanding the mechanisms driving the variation of GHG fluxes across lateral, longitudinal, and temporal dimensions of drying river networks is crucial to better predict river ecosystem contributions to global GHG emissions.

We used an exploratory approach to examine the patterns of GHG fluxes in a river network fragmented by drying. Our first objective (O1) was to determine how river network position, flow permanence and the duration of drying, and their interaction would influence GHG fluxes of dry riverbed sediments in comparison to local scale factors. We expected that dry headwater reaches, particularly those that dried more often or for longer, would have higher GHG fluxes than dry reaches further downstream due to the generally higher OM inputs in headwaters. Our second objective (O2) was to determine how drying had a legacy effect on flowing-condition GHG fluxes. We expected that non-perennial sites would have lower GHG emissions than perennial sites due to the disturbance effect of drying on microbial activity and OM availability. Our third objective (O3) was to compare magnitudes and drivers of GHG fluxes in riparian soils and dry sediments to assess the impacts of drying in the lateral dimension. We expected that riparian soil GHG fluxes would have similar magnitudes and drivers to in-stream fluxes during dry conditions, particularly in the headwaters where lateral connectivity is high.

Methods

Study site and sampling design

The Albarine River drains a 313 km² catchment dominated by forest and agricultural land use of predominantly grasslands/meadows and diverse croplands (EEA 2012) in temperate eastern France (Fig. 1). Due to the dominance of porous karstic bedrock in the headwaters and permeable alluvium along the mainstem of the Albarine River, drying events occur across the network, most frequently in the summer when rainfall cannot compensate for these losses (Datry 2012). The regional climate is temperate oceanic (Köppen climate classification: Cfb) (Beck et al. 2018), with a mean annual temperature of 9.8°C and cumulative annual precipitation of 1734 mm. Twenty sites were selected to capture various flow regimes (*see* Section Determining flow regime) across most major tributaries and along the mainstem of the river. The reach length of each study site was defined as 15 times the bankfull width, with a 50 m minimum and 150 m maximum

(Leopold et al. 2020). Sites were sampled seven times from March to December 2021, on average every 42 d, encapsulating a range of hydrological (dry, flowing, and isolated pools) and other seasonal conditions. *See* Supporting Information Fig. S1 for a summary of mean GHG fluxes per sampling campaign (*Note*: N_2O was measured at only four out of the seven campaigns due to logistical constraints). Due to the small sample size of disconnected pools, we could not determine the covariates of GHG fluxes during this hydrological phase. Each sampling campaign took place over 5–8 consecutive days, during daylight hours. Sites were visited in a different order during each sampling campaign to avoid systematic bias due to the time of day.

Determining flow regime

Sites were distributed with a relatively similar proportion of non-perennial ($n = 9$) and perennial ($n = 11$) reaches. Non-perennial sites were defined as those that dried for at least 1 d per year.
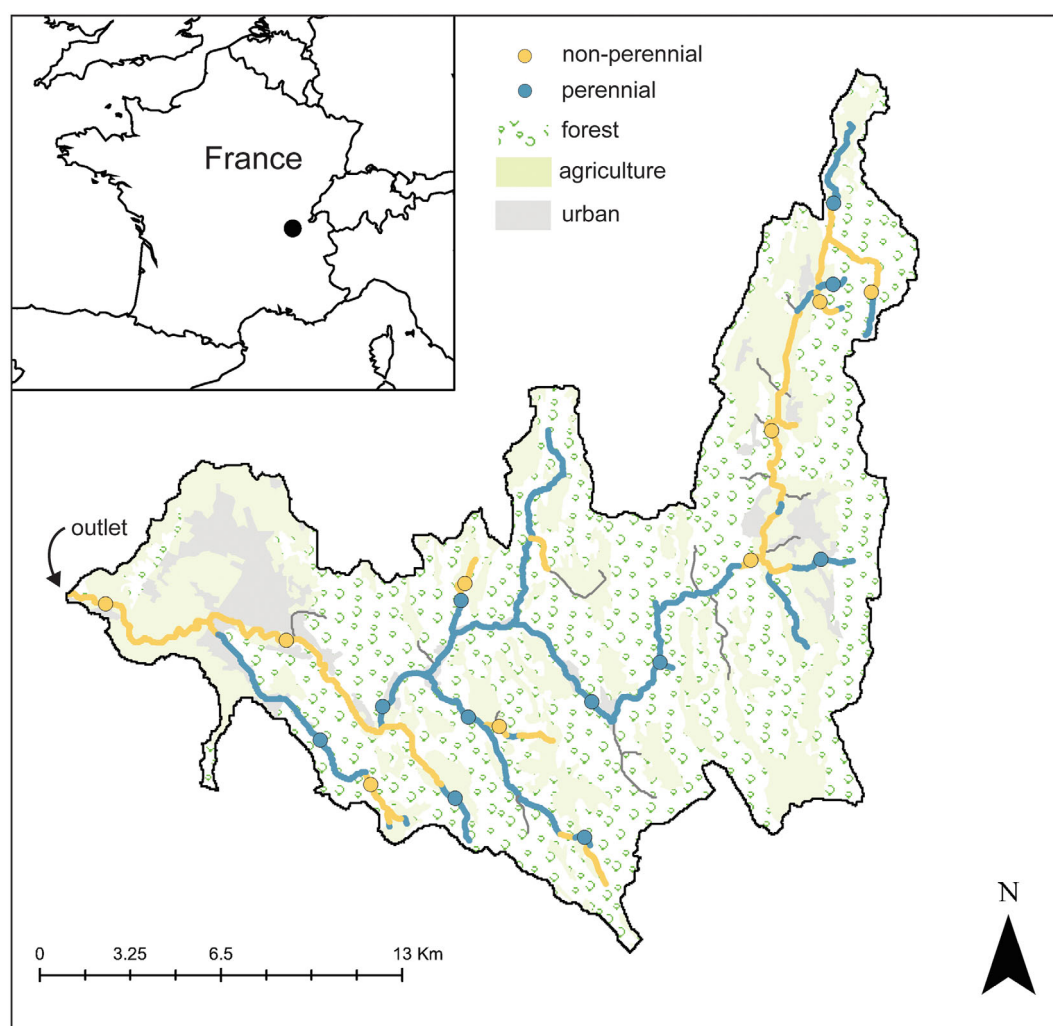
Fig. 1. Map of the Albarine River catchment, France, depicting perennial (blue) and non-perennial (yellow) reaches and sampling sites. The catchment is dominated by forest and agricultural land use, with some urban land use pockets (EEA 2012). Inset map shows the river network location in France. Gray reaches are those with no data on drying.

The sites were selected based on a priori knowledge of the flow regime across the river network (Datry 2012; Gauthier et al. 2020), confirmed by camera trap observations occurring continuously since 2018–2020 (site-dependent). Using daily camera traps (Bushnell Core Dual Sensor, Overland Park, Kansas, United States) photos at non-perennial sites is a proven and effective method for accurately determining hydrological conditions (Kaplan et al. 2019; Noto et al. 2022). The cameras took photos twice per day, once at midday and once at midnight with an infrared flash, to determine the local hydrological conditions. The photos were subsequently manually coded as dry (absence of surface water), flowing, or pooled (disconnected lentic pools) conditions for each day. These photos allowed us to calculate drying metrics such as flow permanence, time since rewetting and time since drying. Time since rewetting and drying were calculated as the number of days elapsed from the last day with nonflowing or flowing conditions, respectively, until the date of sampling. Flow permanence was calculated as the number of days with flowing water, divided by the total number of observations (since the cameras were set up in 2018–2020, site-dependent). We subdivided the non-perennial sites into severe and moderate intermittence: Sites with a flow permanence of < 55% were considered to have severe intermittence ($n = 4$) and sites with a flow permanence of 55–99% were considered to have moderate intermittence ($n = 5$). We measured the distance from each site to its mapped source along the river network (distance to source) in ArcMap (version 10.6.1), which allowed us to calculate the percentage of non-perennial reaches upstream of each site.

GHG fluxes

Five in situ GHG measurements were taken in-stream and in the riparian zone (i.e., the area of direct interaction between terrestrial and aquatic ecosystems; Gregory et al. 1991) at each site and sampling campaign to capture the within-site spatial variability of GHG fluxes. We measured GHG fluxes using a floating chamber designed to reduce turbulence (volume: 3.6 L, area: 0.045 m²; Supporting Information Fig. S2), attached to an anchor for flowing aquatic measurements (Rawitch et al. 2020). Measurements were taken at approximately longitudinally equidistant points, with flowing-condition measurements representative of the pool-riffle sequence of the study reach, but avoiding areas with high turbulence that could disturb the seal between the floating chamber and the water surface. For dry sediment and riparian measurements, a chamber of the same volume and area was placed on top of PVC collars (inner diameter: 24 cm, height: 5 cm for riparian and 7 cm for sediment) permanently installed in the riparian soil (Rochette and Hutchinson 2005), or temporarily sealed with clay on the dry riverbed sediments (Lesmeister and Koschorreck 2017). Riparian soil collars were placed within 2 m from the stream-wetted margin to capture an area within the zone of influence of the stream (Gregory et al. 1991). For isolated pools, a floating chamber was

placed directly onto the water surface. The chambers were connected in a closed loop to portable GHG analyzers to measure CO_2 and CH_4 via cavity ringdown spectroscopy (GasScouter G4301; Picarro) and N_2O via cavity-enhanced absorption (GLA151; ABB-LGR).

We calculated the GHG flux based on the ideal gas law and the linear change in gas concentration over time from measurements recorded every second over an incubation period of ∼ 5 min:

$$F = \frac{dC}{dt} \times \frac{M \times V \times p}{A \times R \times T},$$

where F is the GHG flux (g or mg m^{-2} h^{-1}), dC/dt is the linear slope of gas concentration (μatm) change over time (h), M is the molar mass (g mol^{-1}) of C (for CO_2 and CH_4) or N (for N_2O), V is the chamber headspace volume (L), p is the atmospheric pressure (atm) approximated from local weather station data, A is the area of the chamber (m²), R is the universal gas constant (L atm K^{-1} mol^{-1}), and T is the mean air temperature (K) from data loggers during each measurement. Each time series (CO_2 and CH_4 $n = 1356$ each, N_2O $n = 681$) was visually inspected for quality control, where start and end times were trimmed to exclude any plateaus in concentrations, and any clearly poor quality flux data was removed. Quality control procedures led to the removal of 0.7%, 1%, and 0.3% of all CO_2, CH_4, and N_2O fluxes measured, respectively.

Field environmental measures

Alongside the sampling of GHG fluxes, we measured a suite of environmental parameters at each site at each sampling campaign (Supporting Information Table S1). Air and water temperatures were measured hourly throughout the entire study (iButton dataloggers, Maxim Integrated Products). Soil and sediment temperature and moisture (i.e., volumetric water content) were measured at each GHG measurement point per site (TEROS-11 soil moisture sensor; Meter Group). During flowing conditions, we measured the water depth, width, and velocity (OTT MF Pro flowmeter, HydroMet) at each in-stream GHG measurement. We also measured pH, dissolved oxygen, and conductivity at each site (HQ series multiprobe; Hach Company). Streambed substrate composition (percent bedrock, boulder, gravel, cobble, sand, and silt) and embeddedness (the amount of fine substrate surrounding the coarse substrate of the streambed expressed as %) were estimated visually. We estimated in-stream OM stock from 10 random locations per site using a 0.11 m² quadrat. In dry riverbeds, all visible OM was hand-picked within the quadrat, and in flowing conditions, OM was collected in a driftnet (mesh size = 500 μm) after hand-disturbing the surface of the substrate within the quadrat. Percent canopy cover was visually estimated through a vertical tube (15 cm diameter) at 10 locations per site.

Laboratory environmental measures

For a subset of four of the seven campaigns, we conducted a more in-depth analysis of the soil, sediment, and water for each study site. Data from this subset of sampling campaigns was used to determine the covariates of GHG fluxes. We estimated the sediment and soil OM content from composite ($n = 3$ subsamples) samples taken at a depth of 0–10 cm, sieved to 2 mm, before being dried at 70°C for 24 h and burned at 550°C. We determined sediment pH and conductivity from a 1 : 5 ratio of sediment to deionized water using the same multiprobe as above. Samples for determining the C and N content in soils and sediments were oven-dried, finely ground, and acidified (using 2 N hydrochloric acid). The C and N content was determined using the flash combustion method (Verardo et al. 1990) on a FlashEA 1112 HT Elemental Analyzer (Thermo Electron Corporation). Water chemistry analyses were conducted on stream water samples taken with 60 mL syringes and filtered through 0.2 μm cellulose-acetate filters in acid-washed bottles. Dissolved organic carbon and total dissolved N were measured in a TOC-Analyzer with a nitrogen module (Shimadzu). N-nitrate was measured by ion chromatography (Thermo Fisher Scientific). N-ammonium and soluble reactive phosphorous were determined by colorimetric assays (spectrophotometer U-3900H; Hitachi) using salicylate and the molybdate blue method, respectively. In the laboratory, the OM samples from dry and flowing instream conditions were rinsed and any rocks, sediments, invertebrates, or twigs were removed, leaving predominantly senesced leaf litter. The collected OM was dried at 70°C for 24 h and burned at 550°C to estimate the dry mass and ash-free dry mass, respectively. In June 2022, we collected all of the aboveground detrital and living OM from each permanently installed riparian collar, sorted by type (senesced leaves and needles, woody debris, herbaceous plants, moss, and grass), oven-dried and weighed to determine dry mass as described above.

Statistical analyses

We used a model selection approach to identify the covariates of each GHG across dry sites (O1), perennial sites (O2), non-perennial sites when flowing (O2), and adjacent riparian soils (O3). In each case, we selected the subset of covariates to be included in the saturated linear mixed effects model (LMM) for each GHG in three stages (Table 1; Supporting Information Tables S2, S3). First, we selected variables and their interactions based on our expectations that drying metrics and network location would be important covariates of GHG fluxes. Second, we added variables and their interactions based on a priori knowledge of the drivers of each GHG from the literature. Third, we calculated the correlation coefficients between each GHG and all potential covariates, adding up to three covariates (to limit model complexity) with the highest absolute correlation coefficients and $p < 0.05$. In the final selection, we excluded any covarying explanatory variables

Table 1. Example of the three-step variable selection process for the saturated linear mixed effects model (LMM) to be used in model selection. We included variables based on our research objectives, a priori knowledge, and Pearson's correlation in the saturated model. Here, we show the case of carbon dioxide (CO_2) fluxes from dry riverbed sediments. For the variables included in the other saturated models refer to Supporting Information Tables S2, S3. "×" indicates an interaction term.

Criteria	Dry riverbed CO_2 fluxes
Research objectives	Flowing frequency × distance to source + time since rewetting × distance to source
A priori knowledge	Sediment OM* × distance to source† + OM stock* × distance to source† + sediment OM* × sediment moisture* + sediment OM* × sediment temperature* + sediment moisture* × sediment temperature*
Pearson's correlation	OM stock ($r = 0.48$, $p = 0.0002$) + sediment pH ($r = 0.47$, $p = 0.0002$) + % sand substrate ($r = 0.36$, $p = 0.0002$)

*Keller et al. (2020).
†Richardson et al. (2005).

based on a correlation coefficient > 0.50. We used all data points (not site averages) to have sufficient sample sizes for the saturated models and included a random intercept for the site and a random slope for the campaign to account for the nonindependence of data points. For the LMMs, we used the *lmer* function from the "lme4" R-package (Bates et al. 2015). Using the *dredge* function from the "MuMIn" R-package (Bartoń 2019) we determined the most parsimonious model, as ranked by Akaike's information criterion corrected (AICc) for small sample sizes. All of the models with a difference in AICc < 2 units from the top model were selected and their estimates were averaged (Burnham and Anderson 2004).

To additionally address our second objective (O2) regarding the legacy effect of drying on flowing-condition GHG fluxes, we ran LMMs for each gas, with site average (per sampling campaign) GHG flux as the response variable, flow regime as a fixed factor, and campaign as a random slope. We used a post hoc pairwise comparison of the estimated marginal means using the Tukey HSD method through the *emmeans* function from the "emmeans" R-package (Lenth et al. 2019). To additionally address our third objective (O3) regarding the relationship between dry sediment and riparian soil GHG fluxes, we ran an LMM for each GHG, with site average GHG flux from riparian soils as the response variable and the predictor variables of in-stream GHG flux and its interaction with flow state (i.e., flowing or dry), and distance to source as well as a random slope for the campaign. Although ancillary to our main objectives, to determine the differences in GHG fluxes between habitats, we used LMMs as with flow regime, except with habitat as a fixed factor.

To meet the assumptions of heteroscedasticity and normality of residuals for the LMMs, we applied a log transformation to the response variables and any outlying values according to Cook's distance were removed. If there were negative values in the response variable (y) dataset, we added a constant value (a) so that $\min(y + a) > 0$ before log transforming. Predictor variables were standardized for the LMMs by scaling and centring to reduce the effect of different measurement units and enable ease of interpretation. All statistical analyses were conducted using the statistical software R (version 4.2.2; R Core Team 2023).

Results

GHG fluxes from dry sediments (O1)

Network position, drying metrics, or their interaction did not covary with dry sediment GHG fluxes. Dry sediments were on average a weak source of CO_2 (0.37 ± 0.45 g CO_2-C m^{-2}), CH_4 (0.23 ± 0.88 mg CH_4-C m^{-2} d^{-1}), and N_2O (0.02 ± 0.04 mg N_2O-N m^{-2} d^{-1}; Supporting Information Table S4). Dry sediment CO_2 fluxes positively covaried with sediment moisture, according to the top-ranked models (Fig. 2; Supporting Information Table S5). However, these averaged models had relatively low explanatory power, with a mean R^2 of 0.18. The top model for both dry CH_4 and N_2O fluxes in dry sediments was the null model, with no other model within 2 AICc units. Although ancillary to O1, GHG fluxes from dry sediments were consistently four to 16.5 times lower than from flowing waters (Supporting Information Fig. S3; Supporting Information Tables S4, S6). Where it was possible to identify the covariates of dry sediment GHG fluxes, local factors were more important than network position and drying metrics.

Drying legacy on flowing condition GHG fluxes (O2)

Drying had a legacy effect on the magnitudes of flowing-condition CO_2 fluxes, but a less marked effect on CH_4 and N_2O fluxes. Flowing-condition CO_2 fluxes were 29 times higher from perennial sites than non-perennial sites with severe intermittence (Tukey post hoc pairwise comparison: $\beta = -0.95 \pm 0.36$, $p = 0.02$; Fig. 3; Supporting Information Tables S4, S7, S8). Flowing-condition CH_4 fluxes were not significantly different between perennial (0.63 ± 1.90 mg CH_4-C m^{-2} d^{-1}), moderately intermittent (1.38 ± 3.55 mg CH_4-C m^{-2} d^{-1}), and severely intermittent (1.91 ± 2.76 mg CH_4-C m^{-2} d^{-1}) sites. Flowing-condition N_2O fluxes were four times higher at perennial sites than at sites with severe intermittence (Tukey: $\beta = -0.19 \pm 0.11$, $p = 0.20$) and two times higher at perennial sites than at sites with moderate intermittence (Tukey: $\beta = -0.16 \pm 0.08$, $p = 0.15$), although the means were not identified as statistically different with the given sample size and variation.

The covariates from the top-ranked models for flowing GHG fluxes differed between non-perennial and perennial sites (Fig. 4; Supporting Information Table S9). Flowing-condition CO_2 fluxes at non-perennial sites positively covaried with time since rewetting, embeddedness, and water temperature. At perennial sites, flowing-condition CO_2 fluxes positively covaried with the percentage of non-perennial reaches upstream and sediment OM content, and negatively covaried with OM stock. Flowing-condition CH_4 fluxes at non-perennial sites positively correlated with water temperature and dissolved oxygen. The top model for flowing-condition CH_4 fluxes at perennial sites was the null model, with no other model within 2 AICc units. Flowing-condition N_2O fluxes at non-perennial sites positively covaried with water temperature, a common covariate across all GHGs at flowing non-perennial sites. In addition, N_2O fluxes at non-perennial sites positively covaried with time since

(a) Dry sediments
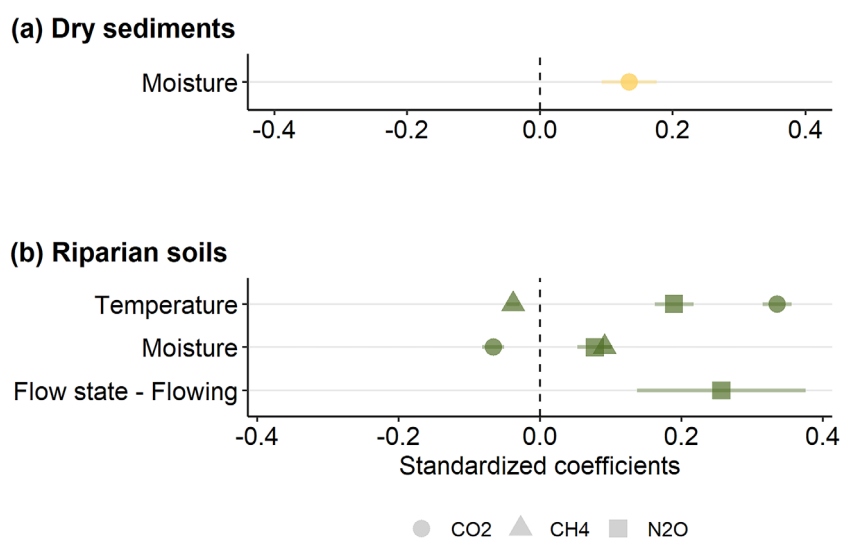
(b) Riparian soils

Fig. 2. Variables from the averaged top models for dry sediment (**a**) and riparian soil (**b**) greenhouse gas fluxes. The top model for CH_4 and N_2O fluxes in dry sediments were the null models, with no other model within 2 AICc units. Error bars represent the standard errors of the coefficients.
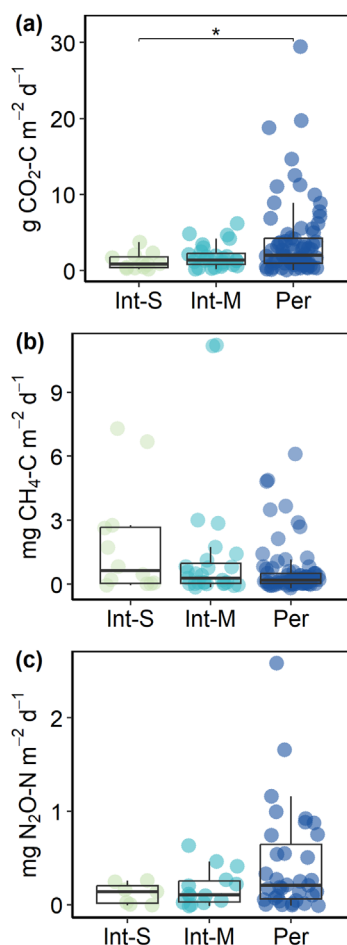
Fig. 3. Site average (per sampling campaign) flowing-condition CO_2 (**a**), CH_4 (**b**), and N_2O (**c**) fluxes across non-perennial sites with severe intermittence (Int-S; $n = 4$), with a flow permanence of < 55%; moderate intermittence (Int-M; $n = 5$), with a flow permanence of 55–99%; and perennial (Per; $n = 11$) sites with a flow permanence of 100%. Box plots display the median, 25th, and 75th percentiles; whiskers display values $1.5\times$ interquartile range. Asterisk indicates pairwise significant difference of estimated means (Tukey HSD) from linear mixed effect models (*$p < 0.05$).

rewetting, distance to the source, velocity, total dissolved N; and negatively covaried with OM stock, N-nitrate, and distance to the source in interaction with OM stock. At perennial sites, N_2O fluxes positively covaried with the percentage of non-perennial reaches upstream, sediment OM, N-nitrate, and total dissolved N (Fig. 4; Supporting Information Table S9).

GHG fluxes from riparian soils (O3)

Riparian soil and dry riverbed sediment GHG fluxes had different magnitudes and covariates. Riparian soil CO_2 and CH_4 fluxes were respectively 6.5 times higher (Tukey post hoc pairwise comparison: $\beta = -0.47 \pm 0.08$, $p < 0.0001$) and 1.8 times lower (Tukey: $\beta = -0.28 \pm 0.05$, $p < 0.0001$) on average than from dry sediments (Supporting Information Tables S4,

S6, S10). N_2O fluxes did not significantly differ between riparian soils (0.13 ± 0.31 mg N_2O-N m^{-2} d^{-1}) and dry sediments (0.02 ± 0.04 mg N_2O-N m^{-2} d^{-1}). Riparian soils were a net sink of CH_4, while the other habitat types were a net source of CH_4, besides isolated pools (Supporting Information Fig. S3; Supporting Information Table S4). Riparian soil GHG fluxes covaried with local-scale factors, principally soil temperature, and soil moisture, were shared covariates for all three GHGs (Fig. 2; Supporting Information Table S5). Riparian soil CO_2 fluxes positively covaried with soil temperature and negatively covaried with soil moisture. Riparian soil CH_4 fluxes had the inverse pattern, as fluxes were negatively covaried with soil temperature and positively covaried with soil moisture. Riparian soil N_2O fluxes positively covaried with soil temperature and soil moisture. Riparian GHG fluxes were not related to instream GHG fluxes, regardless of flow conditions or position in the river network (Supporting Information Table S11). However, N_2O fluxes from riparian soils were higher when the site was flowing than dry, according to the averaged top models (Fig. 2; Supporting Information Table S5).

Discussion

Network-scale drying did not directly influence dry sediment GHG fluxes (O1)

We did not find strong support for the predictions associated with our first objective that network position, drying metrics, and their interaction would be more important than local scale environmental factors in driving dry GHG fluxes from a drying river network. There was no clear effect of flow permanence or dry condition duration on GHG fluxes from dry sediments, despite covering a wide range of flow permanence (18–100% of days with surface flow per year) and days since drying (2–24 d, mean = 9.8). The absence of an observable effect could be because peaks in GHG fluxes upon desiccation can occur during the first hours or days since drying, which we did not capture in our sampling design (average sampling interval every 42 d). For example, a sharp drop in sediment OM content can occur within the first 24–48 h of drying, as oxygenation stimulates mineralization of OM (Gómez et al. 2012). Similarly, CH_4 emissions from sediments peaked within 3 d of desiccation in a mesocosm study (Arce et al. 2021). Nitrification was simulated in the first days of sediment desiccation, peaking at 8 d, attributed to enhanced sediment inorganic N content during desiccation (Gómez et al. 2012). In line with our findings, in a field study of alpine ponds, the time since sediment exposure was not an important driver of CO_2 fluxes, and rather local, sediment characteristic-related factors drove CO_2 fluxes (DelVecchia et al. 2021).

Although the specific drying metrics of flow permanence and dry condition duration did not influence dry riverbed GHG fluxes, drying itself had an impact on GHG fluxes simply through the creation of dry vs. flowing conditions. We observed consistently lower fluxes from dry riverbed
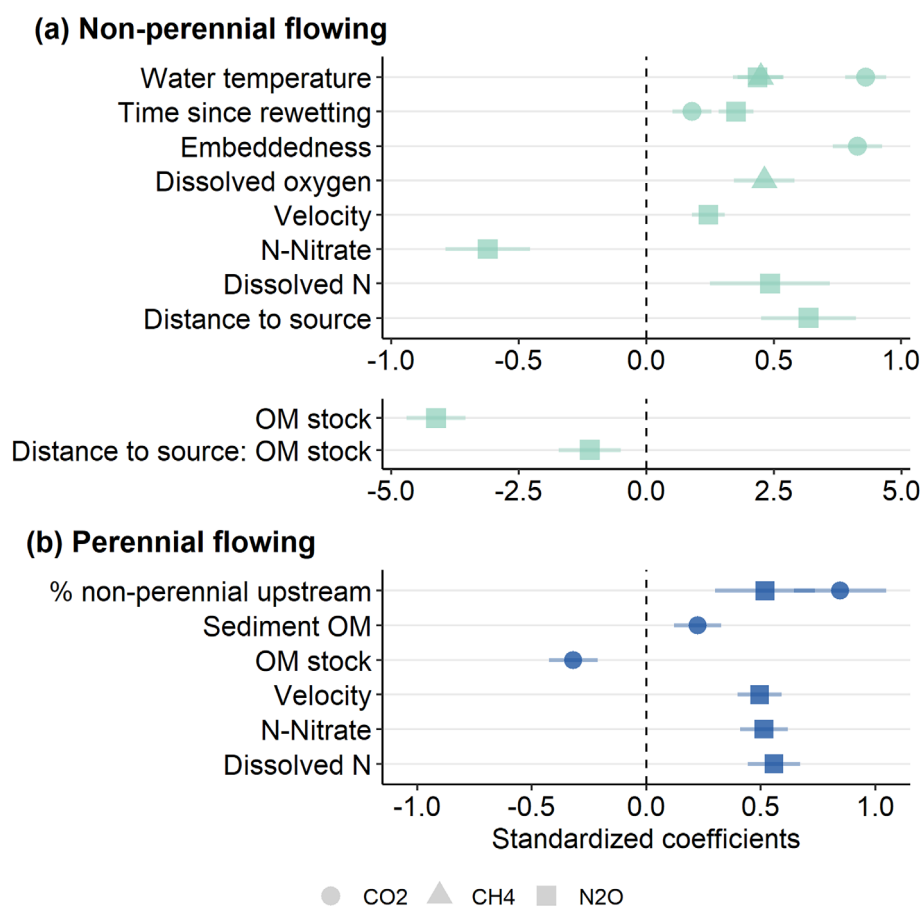
Fig. 4. Variables from the averaged top models for non-perennial flowing (**a**) and perennial flowing (**b**) CO_2, CH_4, and N_2O fluxes. The top model for CH_4 fluxes at perennial sites was the null model, with no other model within 2 AICc units. Error bars represent the standard errors of the coefficients. The scales differ between plots and non-perennial flowing coefficients are separated for better visualization due to the differences in scale.

sediments than from flowing conditions in contrast to previous studies in arid climates, which reported an inverse trend (von Schiller et al. 2014; Gómez-Gener et al. 2015; Looman et al. 2017). Such divergent results may be attributed to different temporal sampling frequencies and scales, and contrasting environmental and climatic conditions compared to previous studies. GHG fluxes are most often measured at the reach scale and by a few snapshots in time, for example, once in the summer (von Schiller et al. 2014), or once during dry conditions and once during flowing conditions (Gómez-Gener et al. 2016). Warm summer temperatures are likely to enhance respiration rates (Lloyd and Taylor 1994), thus possibly resulting in an overestimation of fluxes when compared to cross-seasonal measurements. Temperature was not, however, a driver of dry sediment GHG fluxes in our study, instead, sediment moisture was positively covaried with CO_2 fluxes. Moisture facilitates contact between microorganisms and labile OM (Keller et al. 2020), thus the relatively low concentrations of sediment OM may also possibly explain the relatively low GHG fluxes from dry sediments in our study. Most previous research has been conducted in arid climates (Gallo et al. 2014;

von Schiller et al. 2014; Gómez-Gener et al. 2016; Bolpagni et al. 2017) where respiration rates may be generally higher than in our temperate study region, given the temperature-dependence of respiration rates (Lloyd and Taylor 1994). Microbial communities that are frequently exposed to water stress, such as those in arid climates, may be better adapted to metabolizing under dry conditions than those in temperate climates (Fierer et al. 2003; Arce et al. 2014). Moreover, measurements limited to the reach scale (e.g., Looman et al. 2017), do not account for the high spatial variability in environmental conditions along a river network, and its influence on biogeochemical processes. Accounting for the network-scale spatial variability is important, as many key drivers of riverine GHG fluxes, such as terrestrial OM inputs and groundwater inputs of organic C, vary across the river network (Vannote et al. 1980; Hotchkiss et al. 2015).

We were not able to identify the covariates of CH_4 and N_2O fluxes from dry sediments in our study. The main drivers of CH_4 fluxes from dry riverbeds usually include sediment temperature (Gallo et al. 2014), sediment moisture, and OM content (Paranaíba et al. 2021). N_2O fluxes from freshwater

sediments are principally influenced by water fluctuations, nutrient availability, and oxygen availability (Pinto et al. [2021]). Initial sediment drying may promote N_2O emission through nitrification, while N_2O emissions may decline with prolonged drying as denitrification significantly decreases with decreasing sediment moisture (Gómez et al. [2012]). Although we did not find evidence to support the predictions from our first objective, it is crucial to continue advancing our understanding of the drivers of dry-condition GHG fluxes across drying river networks, especially considering that future climate scenarios predict augmented terrestrial subsidies that can enhance C outgassing from inland waters (Regnier et al. [2022]).

Drying had a spatial and temporal legacy effect on GHG fluxes during flowing conditions (O2)

In partial accordance with our expectations, drying had a network-scale spatial effect on flowing condition CO_2 and N_2O fluxes, but a less marked effect on CH_4 fluxes. CO_2 and N_2O fluxes from perennial sites increased with the percentage of non-perennial reaches upstream, potentially driven by OM inputs from upstream perennial reaches. The importance of OM in stimulating CO_2 emissions at non-perennial reaches was demonstrated in laboratory incubations from a global study (Datry et al. [2018]). Aridity, riparian canopy cover, channel width, and dry phase duration were the main drivers of OM quantity and quality in non-perennial rivers (Datry et al. [2018]). However, this stimulatory effect has yet to be tested in situ, therefore our exploratory findings offer insights for future research, which can test the hypothesis that the accumulation of OM during dry conditions may provide substrate for respiration upon flow resumption to downstream perennial reaches (Catalàn et al. [2023]). The same relationship with the percentage of non-perennial reaches upstream was not observed for CH_4, thus it could be tested to determine whether, under environmental conditions favorable for methanogenesis, an influx of OM from upstream perennial reaches will augment CH_4 emissions.

In addition to a network-scale spatial effect, drying also had a local temporal legacy effect on GHG fluxes during flowing conditions. The evidence was strongest for CO_2, where fluxes in flowing conditions were up to 29 times higher from perennial than non-perennial sites, indicating a negative legacy effect of drying even after flow resumption. Similarly, N_2O fluxes were slightly higher on average (although not significantly) at perennial sites than non-perennial sites, whereas there were no differences in CH_4 fluxes across flow regimes. Lateral hydrological inputs can be an important contributor to GHGs fluxes in streams, during flowing conditions (Hotchkiss et al. [2015]) as well as during drought conditions (Gómez-Gener et al. [2020]). Thus, a potential hypothesis to account for the lower N_2O and CO_2 fluxes in non-perennial sites could be that reduced hydrological connectivity at non-perennial sites (Gómez-Gener et al. [2020]) results in lower inputs of nitrate (Beaulieu et al. [2010]) and C (Gómez-Gener et al. [2020]) from the groundwater. Given that the riparian soils were sinks of

CH_4, it is possible that lateral inputs of CH_4 from soils were less important for this gas, and in situ production was more important, thereby potentially explaining the lack of a difference between flow regimes when compared to CO_2 and N_2O.

At non-perennial sites, CO_2 and N_2O fluxes under flowing conditions increased with time since rewetting, indicating a negative legacy effect of drying on some processes controlling CO_2 and N_2O production or emission, which recovers over time. Moreover, the covariates of the GHGs differed between perennial and non-perennial sites, providing additional support for a potential legacy effect of drying GHG fluxes, as historic drying can alter biotic and abiotic conditions even after flow resumes. For example, drying history impacts invertebrate decomposer (Pinna et al. [2016]; Di Sabatino et al. [2022]) and microbial community (Schreckinger et al. [2022]) structure and functioning, which play key roles in OM decomposition. In the Albarine River, in-stream litter decomposition was still negatively impacted by drying 6 months after flow resumption, with an exponential decline in leaf litter breakdown with decreased flow permanence associated with a decline in invertebrate decomposer assemblages (Datry et al. [2011]). Therefore, the impact of desiccation on in-stream microbial and invertebrate decomposer communities, which recovers with time since rewetting, may have subsequently resulted in lower flowing CO_2 and N_2O fluxes in non-perennial than perennial sites due to a reduced OM processing capacity. We did not observe an effect of time since rewetting on CH_4 fluxes from non-perennial sites, which could be because methanogenic communities may not be as sensitive to drying and oxygen exposure as previously thought (Liu et al. [2022]). Based on our results, future studies could examine the specific mechanisms by which drying has a legacy effect, for example, through downstream transport of OM accumulated in dry reaches, through stress on decomposer communities, or through reduced lateral connectivity.

Riparian soil and dry sediment GHG fluxes did not have similar magnitudes and covariates (O3)

GHG fluxes did not have similar magnitudes and covariates between dry riverbed sediments and riparian soils. However, we did observe a lateral effect of in-stream conditions on N_2O fluxes from riparian soils, where fluxes were higher during flowing conditions than dry conditions. This effect may be a result of a lower water table during dry conditions, reducing soil moisture, and limiting denitrification (Butterbach-Bahl et al. [2013]). We observed sevenfold higher CO_2 fluxes and twofold lower CH_4 fluxes in riparian soils compared to dry riverbed sediments. Generally, soils were a net sink of CH_4, while dry riverbed sediments were a net (weak) source of CH_4, likely due to the higher OM content of soils combined with conditions suitable for methanotrophy. These results are in contrast to other studies that found similar CO_2 fluxes from dry sediments and riparian soils (von Schiller et al. [2014]; Gómez-Gener et al. [2016]). Temperature and moisture tended to be

the top covariates of riparian soil GHG fluxes, and similarly soil moisture covaried with dry sediment CO_2 fluxes. Despite some similar covariates between soils and dry-condition GHG fluxes, the fluxes were not correlated. This lack of correlation may be because these drivers act independently in the riparian zone and in-stream at the same site due to differences in environmental conditions, substrate composition, and microbial community composition. The dry riverbed sediments of our study displayed a low degree of "terrestrialization", or similarity to soils (Arce et al. 2019), possibly due to the relatively short duration of dry conditions, the generally coarse substrate, low OM content, and temperate climate. We observed very limited formation of soil crusts, and dry sites tended to have a very low (if any) vegetative colonization, further differentiating between the riverbed sediments and riparian soils (Arce et al. 2019). Furthermore, canopy cover shading effects on substrate temperature and moisture may be more pronounced in the riparian zone than on in-stream habitats, particularly when the river widens further away from the headwaters. When upscaling GHG fluxes, riparian soils and dry riverbed sediments should be considered separately with respect to their GHG emission potential.

Conclusions

As one of the first studies to measure CO_2, CH_4, and N_2O fluxes across a drying river network at a high spatial and temporal resolution, we advance the understanding of the covariates and magnitudes of GHG fluxes in a non-perennial river network. GHG fluxes were consistently higher from flowing than dry conditions, in contrast with several studies in arid climates. Current global estimates of CO_2 fluxes from dry inland waters may be overestimated as a result of this bias towards measurements in arid regions with relatively high CO_2 fluxes (Marcé et al. 2019). Thus, our study highlights the importance of taking into consideration a geographic diversity of measurements when estimating GHG fluxes from dry riverbed sediments. Local- and network-scale drying had a negative legacy effect on CO_2 fluxes, with up to 29 times higher CO_2 fluxes at perennial than non-perennial sites when flowing. We also found evidence that the longitudinal distribution of drying can impact network-scale CO_2 and N_2O fluxes after flow resumes. The importance of including dry riverbed CO_2 and CH_4 fluxes in the global upscaling of GHG budgets has been previously demonstrated (Keller et al. 2020; Paranaíba et al. 2021), however, N_2O fluxes from dry sediments should additionally be considered, especially given the high global warming potential of N_2O (Myhre et al. 2013). Future studies can examine the relationship between biological decomposer communities and GHG fluxes to better elucidate the mechanisms by which desiccation impacts GHG fluxes in drying river networks. Another important area of continued research is examining the effects of drying on riparian-stream hydrological connectivity and associated lateral inputs of GHGs from terrestrial origins. Our study findings can help to improve global GHG

estimates from river networks, which in large part dry intermittently (Messager et al. 2021), or are likely to become intermittently dry in the face of global change (Döll and Schmied 2012; Pumo et al. 2016; Zipper et al. 2021).

Data availability statement

Data and programming code to replicate analyses and figures are available at: https://github.com/TeresaSilverthorn/GHG_Albarine.

References

Allen, G. H., and T. M. Pavelsky. 2018. Global extent of rivers and streams. Science **361**: 585–588. doi:10.1126/science.aat0636

Arce, M. I., M. del Mar Sanchez-Montoya, M. Rosario Vidal-Abarca, M. Luisa Suarez, and R. Gomez. 2014. Implications of flow intermittency on sediment nitrogen availability and processing rates in a Mediterranean headwater stream. Aquat. Sci. **76**: 173–186. doi:10.1007/s00027-013-0327-2

Arce, M. I., and others. 2019. A conceptual framework for understanding the biogeochemistry of dry riverbeds through the lens of soil science. Earth Sci. Rev. **188**: 441–453. doi:10.1016/j.earscirev.2018.12.001

Arce, M. I., M. M. Bengtsson, D. von Schiller, D. Zak, J. Täumer, T. Urich, and G. Singer. 2021. Desiccation time and rainfall control gaseous carbon fluxes in an intermittent stream. Biogeochemistry **155**: 381–400. doi:10.1007/s10533-021-00831-6

Bartoń, K. 2019. MuMIn: Multi-model inference (R Package Version 1.43.6).

Bates, D., M. Mächler, B. Bolker, and S. Walker. 2015. Fitting linear mixed-effects models using lme. J. Stat. Softw. **67**: 1–48. doi:10.18637/jss.v067.i01

Battin, T. J., L. A. Kaplan, S. Findlay, C. S. Hopkinson, E. Marti, A. I. Packman, J. D. Newbold, and F. Sabater. 2008. Biophysical controls on organic carbon fluxes in fluvial networks. Nat. Geosci. **1**: 95–100. doi:10.1038/ngeo101

Battin, T. J., S. Luyssaert, L. A. Kaplan, A. K. Aufdenkampe, A. Richter, and L. J. Tranvik. 2009. The boundless carbon cycle. Nat. Geosci. **2**: 598–600. doi:10.1038/ngeo618

Battin, T. J., and others. 2023. River ecosystem metabolism and carbon biogeochemistry in a changing world. Nature **613**: 449–459. doi:10.1038/s41586-022-05500-8

Beaulieu, J. J., W. D. Shuster, and J. A. Rebholz. 2010. Nitrous oxide emissions from a large, Impounded River: The Ohio River. Environ. Sci. Technol. **44**: 7527–7533. doi:10.1021/es1016735

Beck, H. E., N. E. Zimmermann, T. R. McVicar, N. Vergopolan, A. Berg, and E. F. Wood. 2018. Present and future Köppen-Geiger climate classification maps at 1-km resolution. Sci. Data **5**: 180214. doi:10.1038/sdata.2018.214

Bolpagni, R., S. Folegot, A. Laini, and M. Bartoli. 2017. Role of ephemeral vegetation of emerging river bottoms in

modulating CO_2 exchanges across a temperate large low-land river stretch. Aquat. Sci. **79**: 149–158. doi:10.1007/s00027-016-0486-z

Burnham, K. P., and D. R. Anderson [eds.]. 2004. Model selection and multimodel inference. Springer.

Butterbach-Bahl, K., E. M. Baggs, M. Dannenmann, R. Kiese, and S. Zechmeister-Boltenstern. 2013. Nitrous oxide emissions from soils: How well do we understand the processes and their controls? Philos. Trans. R. Soc. B Biol. Sci. **368**: 20130122. doi:10.1098/rstb.2013.0122

Catalàn, N., and others. 2023. Pulse, shunt and storage: Hydrological contraction shapes processing and export of particulate organic matter in river networks. Ecosystems. **26**: 873–892. doi:10.1007/s10021-022-00802-4

Cid, N., and others. 2021. From meta-system theory to the sustainable management of rivers in the Anthropocene. Front. Ecol. Environ. **20**: 49–57. doi:10.1002/fee.2417

Cole, J. J., and others. 2007. Plumbing the global carbon cycle: Integrating inland waters into the terrestrial carbon budget. Ecosystems **10**: 172–185. doi:10.1007/s10021-006-9013-8

Covino, T. 2017. Hydrologic connectivity as a framework for understanding biogeochemical flux through watersheds and along fluvial networks. Geomorphology **277**: 133–144. doi:10.1016/j.geomorph.2016.09.030

Datry, T. 2012. Benthic and hyporheic invertebrate assemblages along a flow intermittence gradient: Effects of duration of dry events. Freshw. Biol. **57**: 563–574. doi:10.1111/j.1365-2427.2011.02725.x

Datry, T., R. Corti, C. Claret, and M. Philippe. 2011. Flow intermittence controls leaf litter breakdown in a French temporary alluvial river: The "drying memory". Aquat. Sci. **73**: 471–483. doi:10.1007/s00027-011-0193-8

Datry, T., H. Pella, C. Leigh, N. Bonada, and B. Hugueny. 2016. A landscape approach to advance intermittent river ecology. Freshw. Biol. **61**: 1200–1213. doi:10.1111/fwb.12645

Datry, T., and others. 2018. A global analysis of terrestrial plant litter dynamics in non-perennial waterways. Nat. Geosci. **11**: 497–503. doi:10.1038/s41561-018-0134-4

Datry, T., and others. 2023. Causes, responses, and implications of anthropogenic versus natural flow intermittence in river networks. BioScience **73**: 9–22. doi:10.1093/biosci/biac098

DelVecchia, A. G., S. Gougherty, B. W. Taylor, and S. A. Wissinger. 2021. Biogeochemical characteristics and hydroperiod affect carbon dioxide flux rates from exposed high-elevation pond sediments. Limnol. Oceanogr. **66**: 1050–1067. doi:10.1002/lno.11663

Di Sabatino, A., L. Coscieme, and G. Cristiano. 2022. Effects of antecedent drying events on structure, composition and functional traits of invertebrate assemblages and leaf-litter breakdown in a former perennial river of Central Apennines (Aterno River, Abruzzo, Central Italy). Ecohydrology **15**: e2358. doi:10.1002/eco.2358

Diamond, J. S., G. Pinay, S. Bernal, M. J. Cohen, D. Lewis, A. Lupon, J. Zarnetske, and F. Moatar. 2023. Light and hydrologic connectivity drive dissolved oxygen synchrony in stream networks. Limnol. Oceanogr. **68**: 322–335. doi:10.1002/lno.12271

Döll, P., and H. M. Schmied. 2012. How is the impact of climate change on river flow regimes related to the impact on mean annual runoff? A global-scale analysis. Environ. Res. Lett. **7**: 014037. doi:10.1088/1748-9326/7/1/014037

European Environment Agency (EEA). 2012. Corine land cover. https://land.copernicus.eu/pan-european/corine-land-cover

Fierer, N., J. P. Schimel, and P. A. Holden. 2003. Influence of drying-rewetting frequency on soil bacterial community structure. Microb. Ecol. **45**: 63–71. doi:10.1007/s00248-002-1007-2

Foulquier, A., J. Artigas, S. Pesce, and T. Datry. 2015. Drying responses of microbial litter decomposition and associated fungal and bacterial communities are not affected by emersion frequency. Freshw. Sci. **34**: 1233–1244. doi:10.1086/682060

Gallo, E. L., K. A. Lohse, C. M. Ferlin, T. Meixner, and P. D. Brooks. 2014. Physical and biological controls on trace gas fluxes in semi-arid urban ephemeral waterways. Biogeochemistry **121**: 189–207. doi:10.1007/s10533-013-9927-0

Gauthier, M., B. Launay, G. Le Goff, H. Pella, C. J. Douady, and T. Datry. 2020. Fragmentation promotes the role of dispersal in determining 10 intermittent headwater stream metacommunities. Freshw. Biol. **65**: 2169–2185. doi:10.1111/fwb.13611

Gómez, R., M. Isabel Arce, J. Javier Gómez, and M. del Mar Sánchez-Montoya. 2012. The effects of drying on sediment nitrogen content in a Mediterranean intermittent stream: A microcosms study. Hydrobiologia **679**: 43–59. doi:10.1007/s10750-011-0854-6

Gómez-Gener, L., and others. 2015. Hot spots for carbon emissions from Mediterranean fluvial networks during summer drought. Biogeochemistry **125**: 409–426. doi:10.1007/s10533-015-0139-7

Gómez-Gener, L., and others. 2016. When water vanishes: Magnitude and regulation of carbon dioxide emissions from dry temporary streams. Ecosystems **19**: 710–723. doi:10.1007/s10021-016-9963-4

Gómez-Gener, L., A. Lupon, H. Laudon, and R. A. Sponseller. 2020. Drought alters the biogeochemistry of boreal stream networks. Nat. Commun. **11**: 1795. doi:10.1038/s41467-020-15496-2

Gregory, S. V., F. J. Swanson, W. A. McKee, and K. W. Cummins. 1991. An ecosystem perspective of riparian zones. BioScience **41**: 540–551. doi:10.2307/1311607

Hotchkiss, E. R., R. O. J. Hal, R. A. Sponseller, and D. Butman. 2015. Sources of and processes controlling CO_2 emissions change with the size of streams and rivers. Nat. Geosci. **8**: 696–699. doi:10.1038/ngeo2507

Jacquet, C., F. Munoz, N. Bonada, T. Datry, J. Heino, and F. Jabot. 2022. Disturbance-driven alteration of patch

connectivity determines local biodiversity recovery within metacommunities. Ecography **2022**: e06199. doi:10.1111/ecog.06199

Kaplan, N. H., E. Sohrt, T. Blume, and M. Weiler. 2019. Monitoring ephemeral, intermittent and perennial streamflow: A data set from 182 sites in the Attert catchment, Luxembourg. Earth Syst. Sci. Data **11**: 1363–1374. doi:10.5194/essd-11-1363-2019

Keller, P. S., and others. 2020. Global CO_2 emissions from dry inland waters share common drivers across ecosystems. Nat. Commun. **11**: 2126. doi:10.1038/s41467-020-15929-y

Kosten, S., S. van den Berg, R. Mendonça, J. R. Paranaíba, F. Roland, S. Sobek, J. Van Den Hoek, and N. Barros. 2018. Extreme drought boosts CO_2 and CH_4 emissions from reservoir drawdown areas. Inland Waters **8**: 329–340. doi:10.1080/20442041.2018.1483126

Leigh, C., and T. Datry. 2017. Drying as a primary hydrological determinant of biodiversity in river systems: A broad-scale analysis. Ecography **40**: 487–499. doi:10.1111/ecog.02230

Lenth, R., H. Singmann, J. Love, P. Buerkner, and M. Herve. 2019. R package emmeans: Estimated marginal means.

Leopold, L. B., M. G. Wolman, and J. P. Miller. 2020. Fluvial processes in geomorphology, 2nd ed. Dover Publications.

Lesmeister, L., and M. Koschorreck. 2017. A closed-chamber method to measure greenhouse gas fluxes from dry aquatic sediments. Atmos. Meas. Tech. **10**: 2377–2382. doi:10.5194/amt-10-2377-2017

Liu, T., X. Li, S. S. Yekta, A. Björn, B.-Z. Mu, L. S. M. Masuda, A. Schnürer, and A. Enrich-Prast. 2022. Absence of oxygen effect on microbial structure and methane production during drying and rewetting events. Sci. Rep. **12**: 16570. doi:10.1038/s41598-022-20448-5

Lloyd, J., and J. A. Taylor. 1994. On the temperature dependence of soil respiration. Funct. Ecol. **8**: 315–323. doi:10.2307/2389824

Looman, A., D. T. Maher, E. Pendall, A. Bass, and I. R. Santos. 2017. The carbon dioxide evasion cycle of an intermittent first-order stream: Contrasting water-air and soil-air exchange. Biogeochemistry **132**: 87–102. doi:10.1007/s10533-016-0289-2

Lupon, A., L. Gómez-Gener, M. L. Fork, H. Laudon, E. Martí, W. Lidberg, and R. A. Sponseller. 2023. Groundwater-stream connections shape the spatial pattern and rates of aquatic metabolism. Limnol. Oceanogr.: Lett. **8**: 350–358. doi:10.1002/lol2.10305

Marcé, R., B. Obrador, L. Gómez-Gener, N. Catalán, M. Koschorreck, M. I. Arce, G. Singer, and D. von Schiller. 2019. Emissions from dry inland waters are a blind spot in the global carbon cycle. Earth Sci. Rev. **188**: 240–248. doi:10.1016/j.earscirev.2018.11.012

Messager, M. L., and others. 2021. Global prevalence of non-perennial rivers and streams. Nature **594**: 391–397. doi:10.1038/s41586-021-03565-5

Myhre, G., and others. 2013. Anthropogenic and natural radiative forcing, p. 659–740. *In* T. F. Stocker and others [eds.], Climate change 2013: The physical science basis. Contribution of working group I to the fifth assessment report of the intergovernmental panel on climate change. Cambridge Univ. Press.

Noto, S., F. Tauro, A. Petroselli, C. Apollonio, G. Botter, and S. Grimaldi. 2022. Low-cost stage-camera system for continuous water-level monitoring in ephemeral streams. Hydrol. Sci. J. **67**: 1439–1448. doi:10.1080/02626667.2022.2079415

Paranaíba, J. R., and others. 2021. Cross-continental importance of CH_4 emissions from dry inland-waters. Sci. Total Environ. **814**: 151925. doi:10.1016/j.scitotenv.2021.151925

Pinna, M., G. Marini, G. Cristiano, L. Mazzotta, P. Vignini, B. Cicolani, and A. Di Sabatino. 2016. Influence of aperiodic summer droughts on leaf litter breakdown and macroinvertebrate assemblages: Testing the drying memory in a Central Apennines River (Aterno River, Italy). Hydrobiologia **782**: 111–126. doi:10.1007/s10750-016-2854-z

Pinto, R., G. Weigelhofer, A. G. Brito, and T. Hein. 2021. Effects of dry-wet cycles on nitrous oxide emissions in freshwater sediments: A synthesis. PeerJ **9**: e10767. doi:10.7717/peerj.10767

Pumo, D., D. Caracciolo, F. Viola, and L. V. Noto. 2016. Climate change effects on the hydrological regime of small non-perennial river basins. Sci. Total Environ. **542**: 76–92. doi:10.1016/j.scitotenv.2015.10.109

R Core Team. 2023. R: A language and environment for statistical computing.

Rawitch, M. J., G. L. Macpherson, and A. E. Brookfield. 2020. The validity of floating chambers in quantifying CO_2 flux from headwater streams. J. Water Clim. Change **12**: 453–468. doi:10.2166/wcc.2020.199

Raymond, P. A., and others. 2013. Global carbon dioxide emissions from inland waters. Nature **503**: 355–359. doi:10.1038/nature12760

Regnier, P., L. Resplandy, R. G. Najjar, and P. Ciais. 2022. The land-to-ocean loops of the global carbon cycle. Nature **603**: 401–410. doi:10.1038/s41586-021-04339-9

Richardson, J. S., R. E. Bilby, and C. A. Bondar. 2005. Organic matter dynamics in small streams of the Pacific Northwest. J. Am. Water Resour. Assoc. **41**: 921–934. doi:10.1111/j.1752-1688.2005.tb03777.x

Rochette, P., and G. L. Hutchinson. 2005. Measurement of soil respiration in situ: Chamber techniques, p. 247–286. *In* Micrometeorology in agricultural systems, v. **47**. American Society of Agronomy.

Schreckinger, J., M. Mutz, C. Mendoza-Lera, and A. Frossard. 2021. Attributes of drying define the structure and functioning of microbial communities in temperate riverbed sediment. Front. Microbiol. **12**: 676615. doi:10.3389/fmicb.2021.676615

Schreckinger, J., M. Mutz, and C. Mendoza-Lera. 2022. When water returns: Drying history shapes respiration and

nutrients release of intermittent river sediment. Sci. Total Environ. **838**: 155950. doi:10.1016/j.scitotenv.2022.155950

Shumilova, O., and others. 2019. Simulating rewetting events in intermittent rivers and ephemeral streams: A global analysis of leached nutrients and organic matter. Glob. Change Biol. **25**: 1591–1611. doi:10.1111/gcb.14537

Truchy, A., and others. 2020. Habitat patchiness, ecological connectivity and the uneven recovery of boreal stream ecosystems from an experimental drought. Glob. Change Biol. **26**: 3455–3472. doi:10.1111/gcb.15063

Vannote, R. L., G. W. Minshall, K. W. Cummins, J. R. Sedell, and C. E. Cushing. 1980. The river continuum concept. Can. J. Fish. Aquat. Sci. **37**: 130–137. doi:10.1139/f80-017

Verardo, D. J., P. N. Froelich, and A. McIntyre. 1990. Determination of organic carbon and nitrogen in marine sediments using the Carlo Erba NA-1500 analyzer. Deep-Sea Res. A: Oceanogr. Res. Pap. **37**: 157–165. doi:10.1016/0198-0149(90)90034-S

von Schiller, D., R. Marcé, B. Obrador, L. Gómez-Gener, J. P. Casas-Ruiz, V. Acuña, and M. Koschorreck. 2014. Carbon dioxide emissions from dry watercourses. Inland Waters **4**: 377–382. doi:10.5268/IW-4.4.746

Wang, F., S. C. Maberly, B. Wang, and X. Liang. 2018. Effects of dams on riverine biogeochemical cycling and ecology. Inland Waters **8**: 130–140. doi:10.1080/20442041.2018.1469335

Zipper, S. C., and others. 2021. Pervasive changes in stream intermittency across the United States. Environ. Res. Lett. **16**: 084033. doi:10.1088/1748-9326/ac14ec

Acknowledgments

Conflict of Interest

The authors declare no conflicts of interest associated with this publication.